CONF-751101--73

ANL/RAS 76-11

F1 PHENOMENOLOGICAL TEST ON FUEL MOTION

(INTERIM REPORT)

MASTER

by

R. G. Palm, S. M. Gehl, R. R. Stewart,

A. De Volpi, and A. B. Rothman

March 1976

*Contents of this report were presented at the Annual Meeting of the American Nuclear Society in San Francisco, November, 1975.

Reactor Analysis and Safety Division
ARGONNE NATIONAL LABORATORY
9700 South Cass Avenue
Argonne, Illinois 60439

ANL/RAS 76-11

F1 PHENOMENOLOGICAL TEST ON FUEL MOTION

(INTERIM REPORT)

by

R. G. Palm, S. M. Gehl, R. R. Stewart,

A. De Volpi, and A. B. Rothman

March 1976

*Contents of this report were presented at the Annual Meeting of the American Nuclear Society in San Francisco, November, 1975.

NOTICE: This informal document contains preliminary information prepared primarily for interim use in fast breeder reactor programs in the U.S. Since it does not constitute a final report, it should be cited as a reference only in special circumstances, such as requirements for regulatory needs.

Reactor Analysis and Safety Division
ARGONNE NATIONAL LABORATORY
9700 South Cass Avenue
Argonne, Illinois 60439

TABLE OF CONTENTS

LIST OF TABLES

LIST OF FIGURES

LIST OF FIGURES (Cont'd)

1.0 SUMMARY

TREAT F-series tests are being conducted to provide data on fuel motion in an LMFBR during a hypothetical loss-of-flow accident. Fuel and fuel boundary conditions in an LMFBR subassembly following sodium voiding and dryout under loss-of-flow conditions are simulated in each F-series test. Simulation is achieved with a single fuel element surrounded by an annular nuclear heated wall in a dry (no sodium) test capsule. Test F1 was conducted with an irradiated fuel element to investigate the effect of fission gas on fuel motion at design power levels following clad melting and drainage.

Prior irradiation of the F1 test fuel element was in EBR-II subassembly X096 (HEDL N-E) at a peak power rating and burnup of 12.0 KW/ft and 2.35 a/o respectively. The fuel contained three structural zones and a central void. An annular W-UO_2 cermet nuclear heated wall surrounded the fuel element along the 13.5 in. fuel column. The nuclear heated wall prevented non-prototypical fuel or clad radial freezeout, and provided a well defined geometry for fuel motion. Selection of the area inside the heated wall was made to be representative of the area inside the perimeter of an LMFBR coolant channel.

Scram of the F1 TREAT transient occurred 14.3 seconds after initiation. The final 10 seconds of the transient was conducted at constant reactor power and generated approximately 11.6 kW/ft (peak) in the test fuel. Axial fuel motion downward was first detected 13.2 seconds after transient initiation by the fast neutron hodoscope. No net upward fuel motion was detected at any time by the hodoscope. The hodoscope observed the fuel motion until 18.5 seconds after transient initiation; one-half of the fuel motion observed by the hodoscope occurred before reactor scram at 14.3 seconds. Final arrangement of the test fuel was indicated by metallographic examination and posttest neutron radiography. Metallographic examination and posttest neutron

radiography showed that extensive fuel melting and axial fuel draining occurred. The fuel draining created a 6 in. axial region voided of fuel above a 5 in. axial region filled with fuel out to the inner surface of the heated wall. No molten fuel moved beyond the ends of the original fuel column. Extensive fuel swelling prior to gross axial fuel motion, and the presence of metallic phases in the molten fuel were significant features of the posttest metallography.

2.0 HARDWARE DESCRIPTION

The test vehicle for the F-series tests is a modified Mark-II loop body illustrated in Fig. 1. A single test fuel pin is in a sealed capsule which is located at one end of the test train. The test train is inserted into the loop from the top and sealed to the loop at the test train flange. Fig. 1 shows that the 13.5 in. long test fuel column is approximately centered in the 48 in. high TREAT core. A B_6Si thermal-neutron filter equivalent to 18 mils thickness covers the outside of the loop body as illustrated. The purpose of the filter is to harden the TREAT neutron spectrum sufficiently to achieve the desired progression of melting in the cladding and fuel, prior to their motion in the test assembly. Dysprosium flux shaping collars were installed on the outside of the neutron filters in order to shape the test fuel axial power profile to that of EBR-II, the prior source of irradiation of the F-series fuel pins. When the Mark-II loop body is used for tests having flowing sodium, an electromagnetic pump is placed between the upper and lower bends. In the F-series, these bends were flanged off as indicated in Fig. 1. A burst disc was incorporated in the F-series loop to vent the loop to the dump tank if high loop pressure were to develop. Fig. 2 is an axial view of the F-series capsule located inside the Mark-II loop. Reference between Figs. 1 and 2 may be made by locating the upper bend of the Mark-II loop and the fuel column in each illustration. Fig. 2 was made to scale axially but not radially. The test fuel pin is located at the radial center of the sealed capsule. Axial motion of the fuel pin is constrained by a tungsten pin through the lower fuel pin end plug, and a fuel pin retainer on the top end plug. Note that the fuel pin retainer restricts downward but not upward movement of the top end plug. The fuel pin is surrounded radially by a W-UO_2 cermet (nuclear heated wall), a thin molybdenum reflector, a

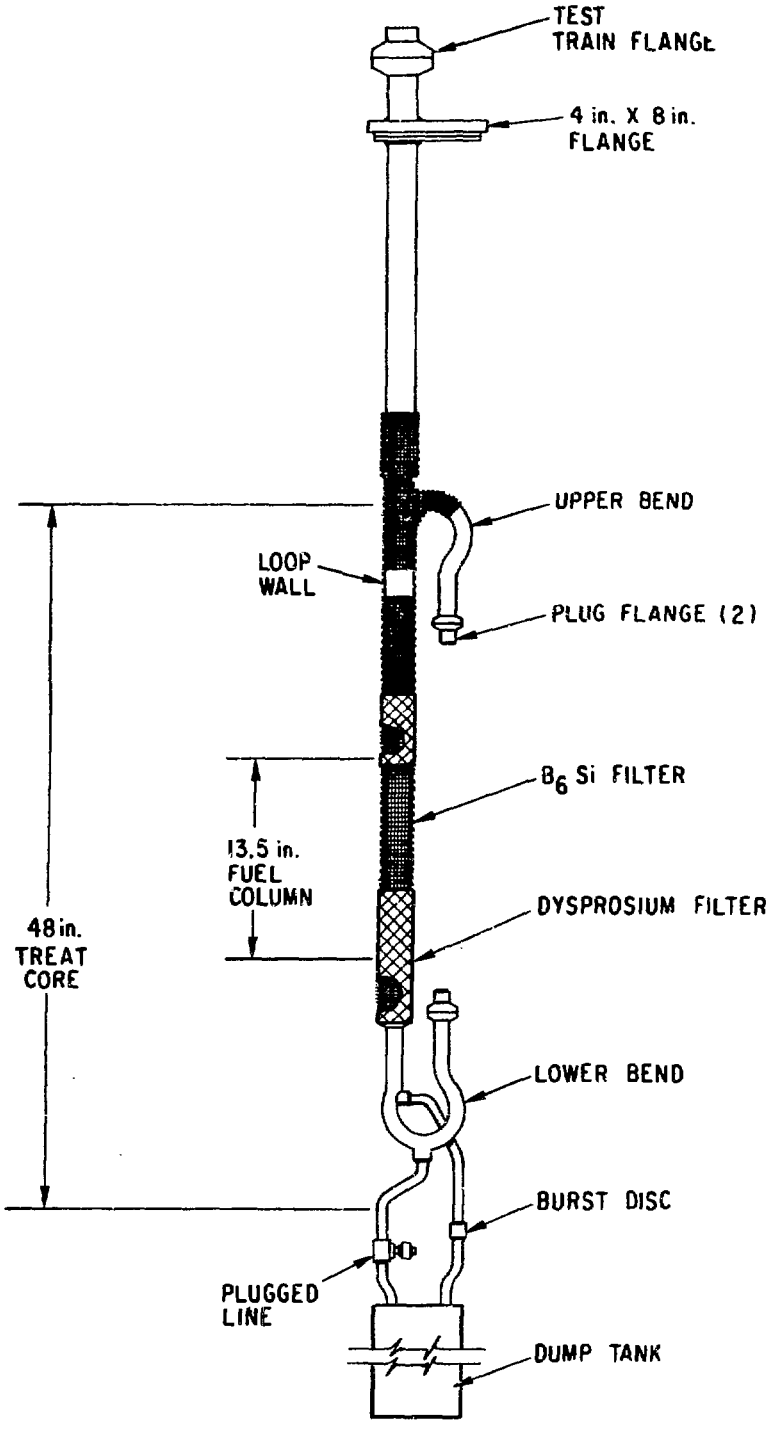

Fig. 1 F-Series Mark-II Loop

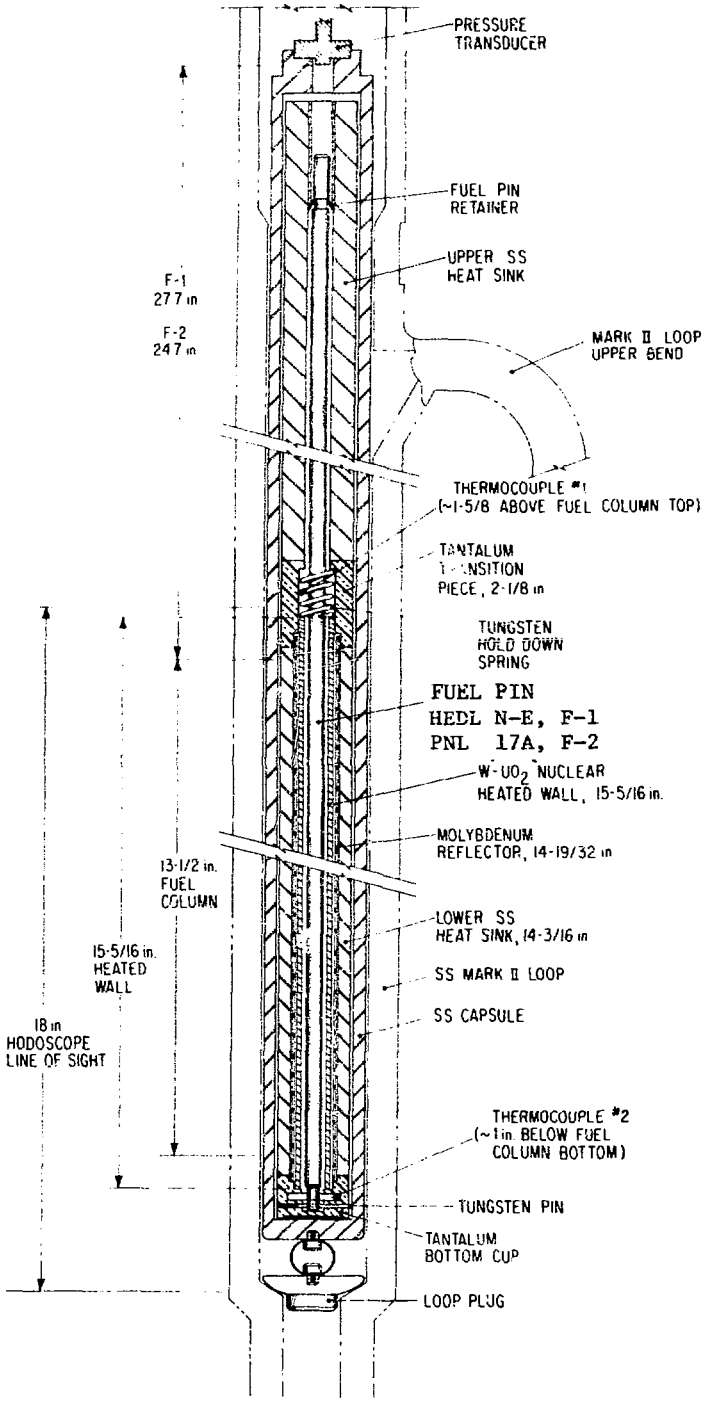

Fig. 2 F-Series Test Capsule

stainless steel heat sink, and a stainless steel capsule wall. A scaled radial cross-section with dimensions of the F-series capsule and loop in the fueled region is shown in Fig. 3. Fig. 2 indicates that the heated wall extends 1 in. above the top of the fuel column and 13/16 in. below the fuel column for a total length of 15 5/16 in. Two large tantalum pieces are located just beyond the ends of the fuel column. These pieces contain and align the heated wall; and in addition, the lower piece serves as a fuel catcher. Thermocouples 1 and 2 are located as shown just above and below the fuel column, respectively. These are type K, 40 mil stainless steel sheathed, Chromel-Alumel thermocouples. The capsule was filled with Ar-3% He to 12.1 psia before each test. The pressure transducer (CEC model A-316 unbonded strain gauge type, $\pm$ 100 psi linear range) is located at the top of the capsule. Fig. 1 shows that the distance from the top of the fuel column to the pressure transducer diaphragm is 27.7 in. long in the F1 test. The fast-neutron hodoscope line of sight is also shown in Fig. 2. It extends 1 1/4 in. above the original top of the test pin fuel column to 3 1/4 in. below the test pin fuel column. Fuel motion is continuously monitored by the fast-neutron hodoscope which was the principal test instrument for the F-series. Fig. 4 shows the F1 test pin. The pin was modified to fit into the F-series test capsule by shortening the bottom end plug and drilling a hole through it for the tungsten locking pin. Note also that the spiral wire wrap was removed from the fuel pin. Table I summarizes data on the F1 fuel pin. Note that the F1 fuel pin plenum pressure was reduced to 12.1 psig and resealed with 99% Xe, 1% He, prior to the test.

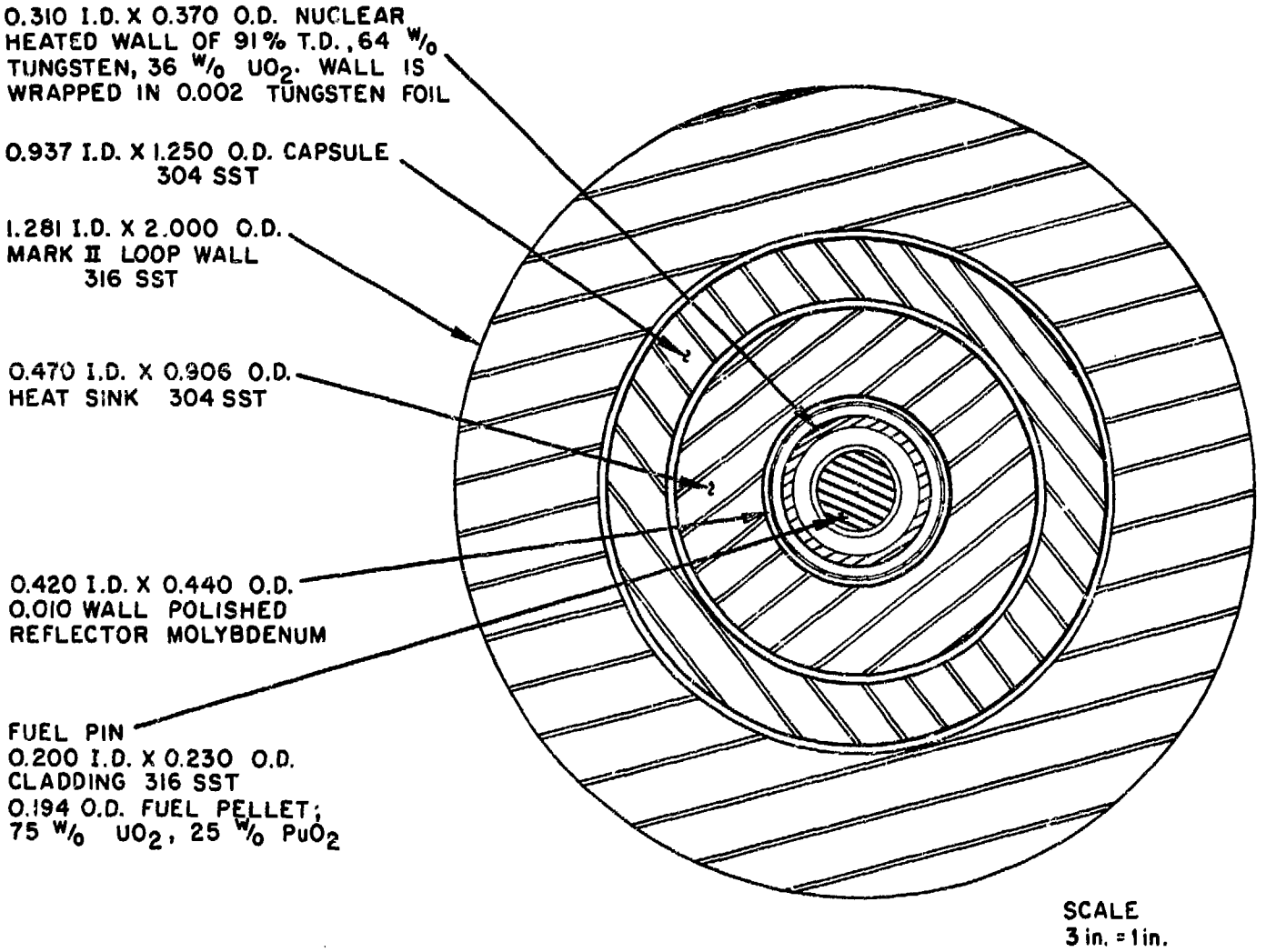

Fig. 3 F-Series Cross Section Through Test Fuel

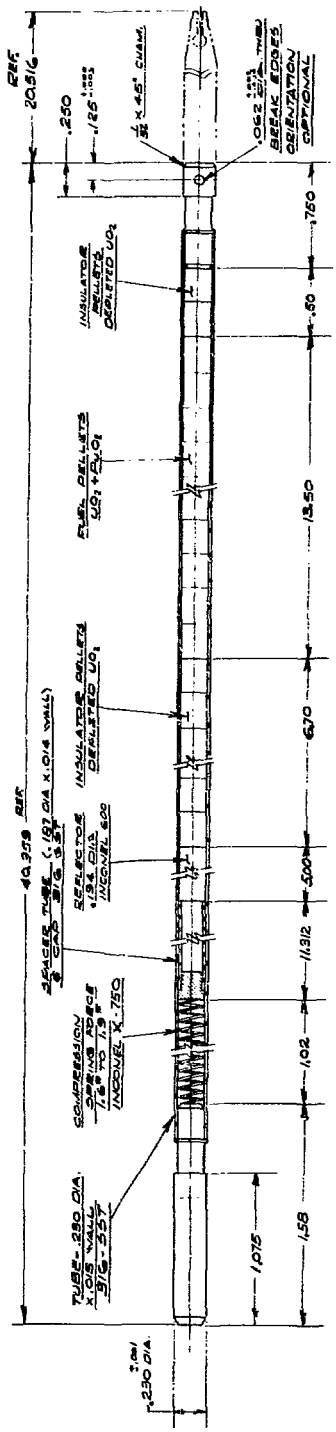

Fig. 4 Fl Fuel Element, HEDL N-E

TABLE I

Fl Fuel Pin Description

Type	HEDL N-E
Pin Number	N-077
Irradiated	in EBR-II
Irradiated Peak Power	12.0 kW/ft
Irradiated Peak Burnup	2.35 a/o
Preirradiation Composition	75% UO_2 - 25% PuO_2
U^{235} Enrichment	77 a/o
Fuel Column Axial Length	13.5 in.
Fuel Microstructural Dimensions (From Sibling Pins at Mid-Axis)	
Central Void Radius	16 mils
Columnar Region Radius	65 mils
Equiaxed Region Radius	68 mils
Unrestructured Region Radius	100 mils
Clad Dimensions	
Inner Radius	100 mils
Outer Radius	115 mils
Fl Plenum Gas Composition	99% Xe, 1% He
Fl Plenum Gas Pressure	12.1 psig

3.0 POWER GENERATION

The peak linear power rating of the test pin during the F1 test is presented in Fig. 5. Fig. 5 is based upon data from F-series power calibration experiments, and the actual F1 test power generation. Fig. 5 was constructed without considering power generation changes due to changes in fuel geometry after gross axial fuel motion begins at ~13 sec in the F1 test. Fig. 6 is the relative axial test pin power generation determined by radiochemistry on fuel used in a calibration transient; this figure is normalized, so the relative peak axial power is unity. Relative fuel radial power generation recommended for the F-series is shown in Fig. 7. The radial power profile is based upon radiochemistry performed on concentric cores of a few fuel pellets irradiated in a fueled calibration transient. Cores from the pellets were obtained by an ultrasonic trepanning technique developed by Yaggee[1]. Note that the calibration fuel pellets did not have central voids, but the test fuel pellets had central voids.

The peak linear power rating for the nuclear heated wall was 8.30 kW/ft in the nominally flattop power portion of the F1 test transient, as determined by radiochemistry in a calibration transient. Note that this power rating only applies for times before gross axial test fuel motion. The same axial power shape used for the test fuel is recommended for the heated wall. A ratio of 1.07 was used to describe the ratio of power generation in the outer half of the heated wall compared to the inner half. This ratio was based upon transport calculations performed for the F-series.

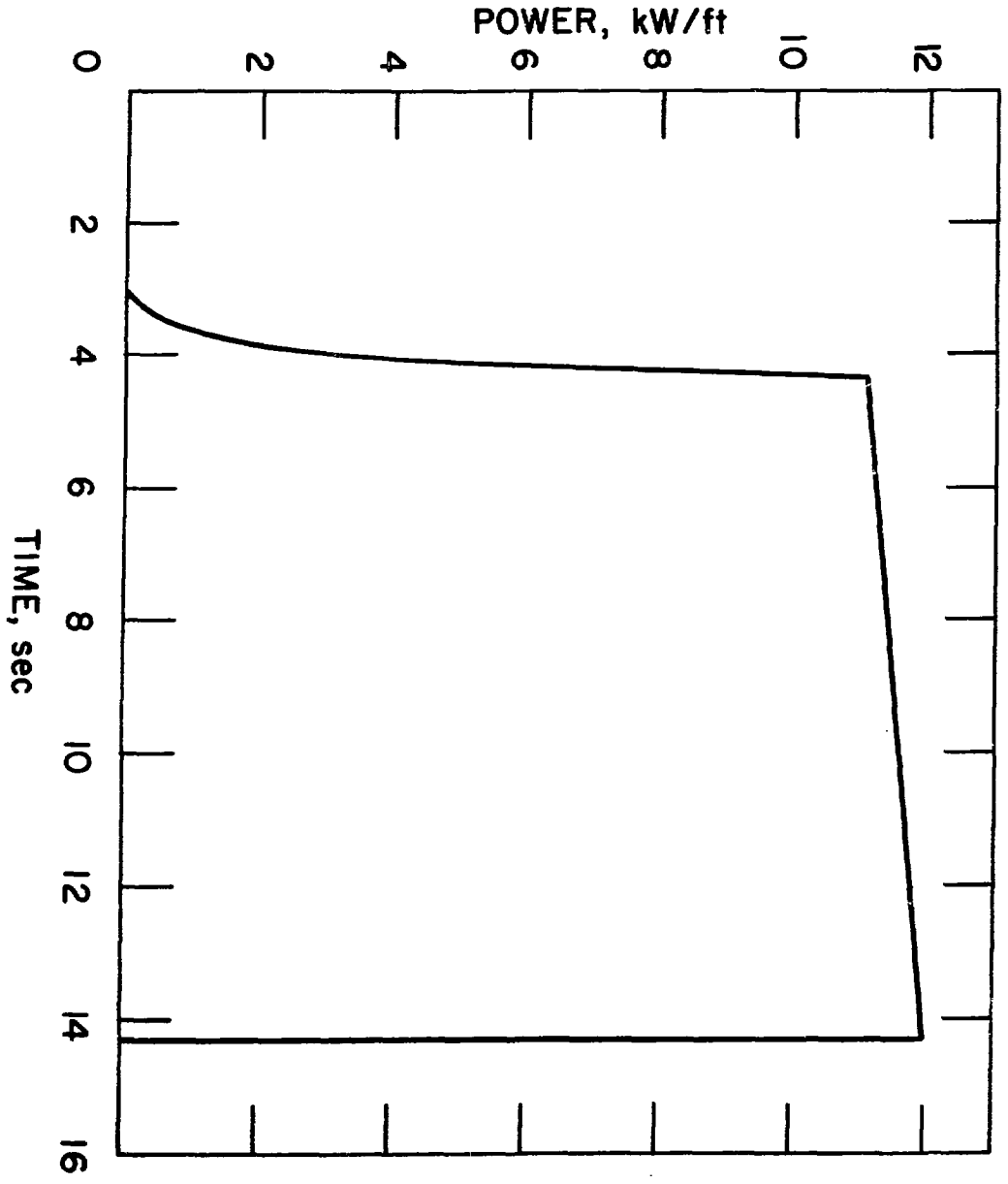

Fig. 5 F1 Test Pin Axial Peak Power Generation

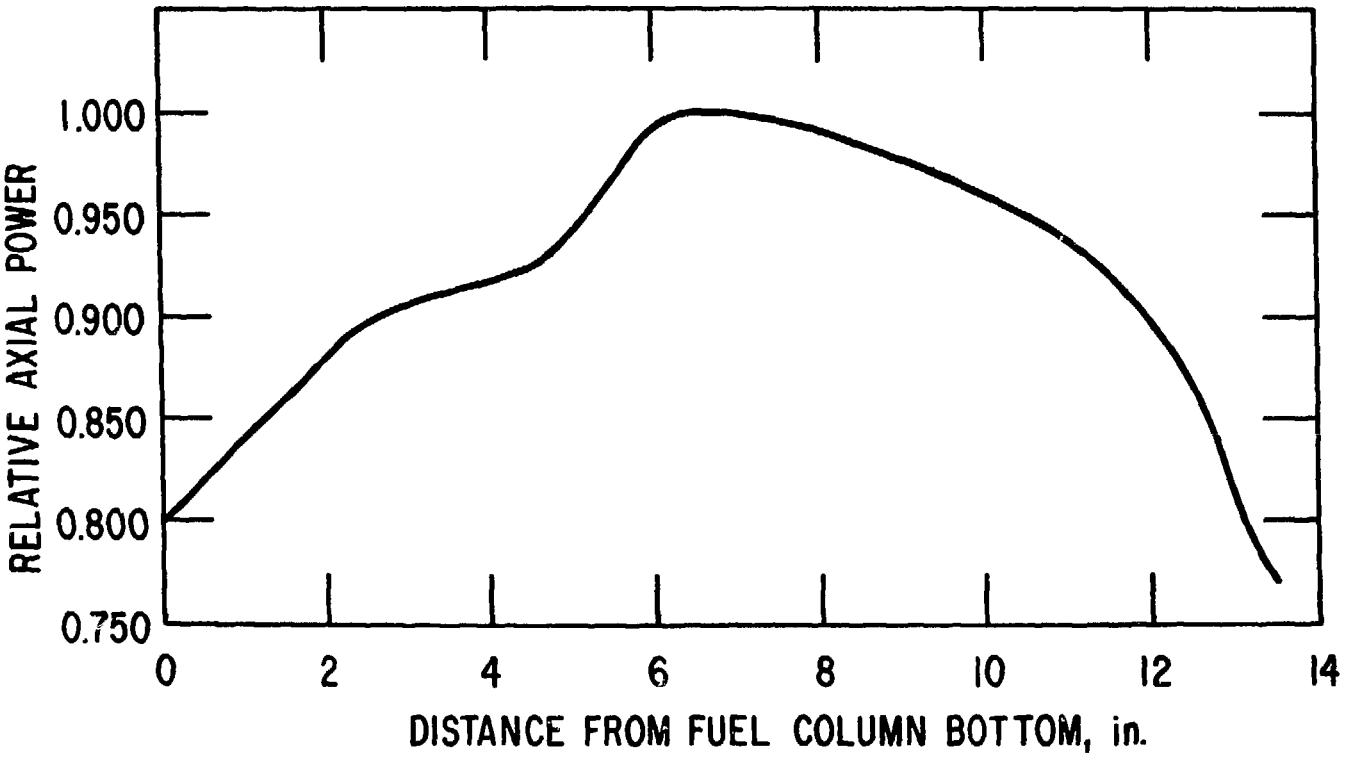

Fig. 6 F-Series Axial Power Distribution from Experiment

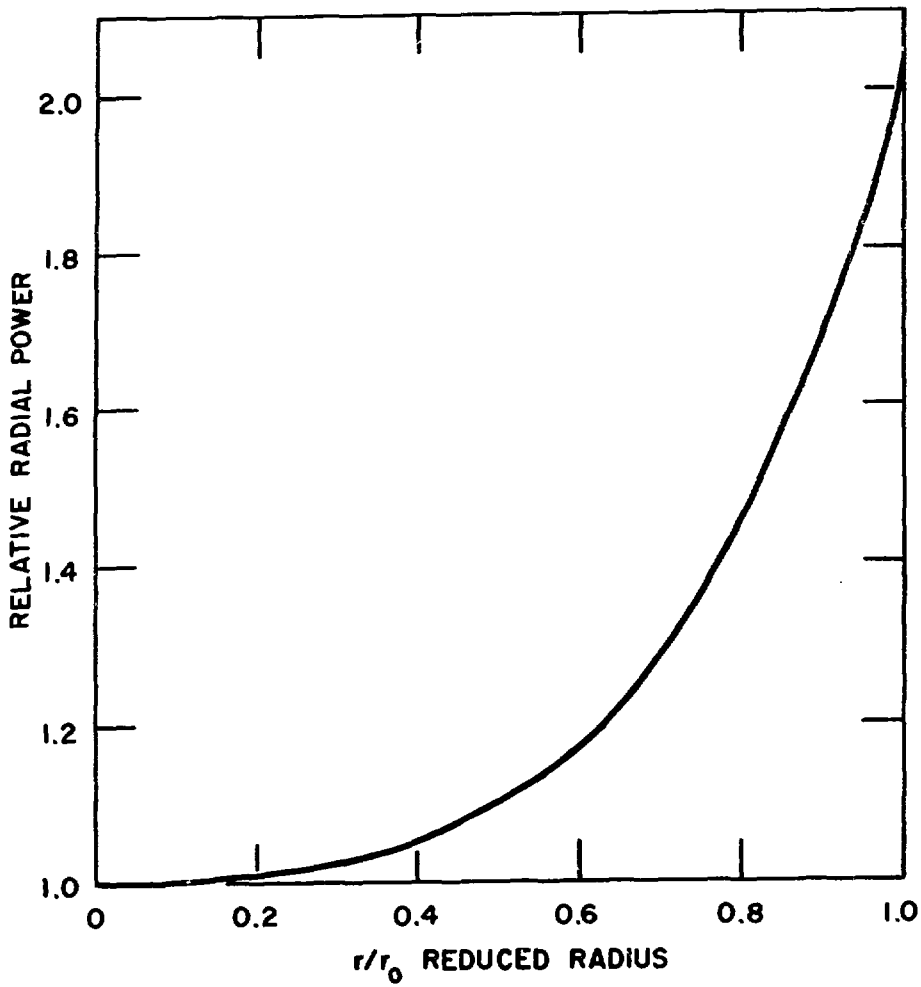

Fig. 7 F-Series Radial Power Profile From Experiment on Unrestructured Fuel (r_o is Outside Radius of Fuel)

4.0 RESULTS

4.1 Test Capsule Data

Fig. 8 summarizes the test capsule data during and just after the F1 test. Data from the two thermocouples, the pressure transducer, and an idealized TREAT power trace are presented with a common time abscissa in Fig. 8.

Neither thermocouple appears to have been contacted by hot clad or fuel in the F1 test, although the upper thermocouple exhibited some interesting behavior. The lower thermocouple (TC-2) exhibits a continuous temperature rise during and just after the period of constant TREAT power. The upper thermocouple (TC-1) rises at a faster rate than the lower thermocouple from 5 to 6.5 sec. After 6.5 sec TC-1 rises at a lower rate than TC-2. The initial faster heatup of the upper thermocouple compared to the lower thermocouple could be explained by the establishment of upward convection currents of capsule fill gas. By 6.5 sec the convection currents had started to diminish. Note that TC-1 also exhibited two separate pauses in temperature rise at 8.5 and 11 sec. It is possible that these pauses are due to some disturbance in heat transfer by convection associated with motion resulting from clad melting, and runoff; or incipient fuel motion.

The capsule pressure exhibits a generally smooth rise over the period of constant TREAT power. This pressure response can be explained by heatup of the test capsule fill gas. No sign of an abrupt or even a gradual release of fission gas into the capsule is apparent from the pressure transducer data. Evidently, the presence of a much larger amount of capsule fill gas compared to fission gas released by the fuel masked the detection of fission gas release.

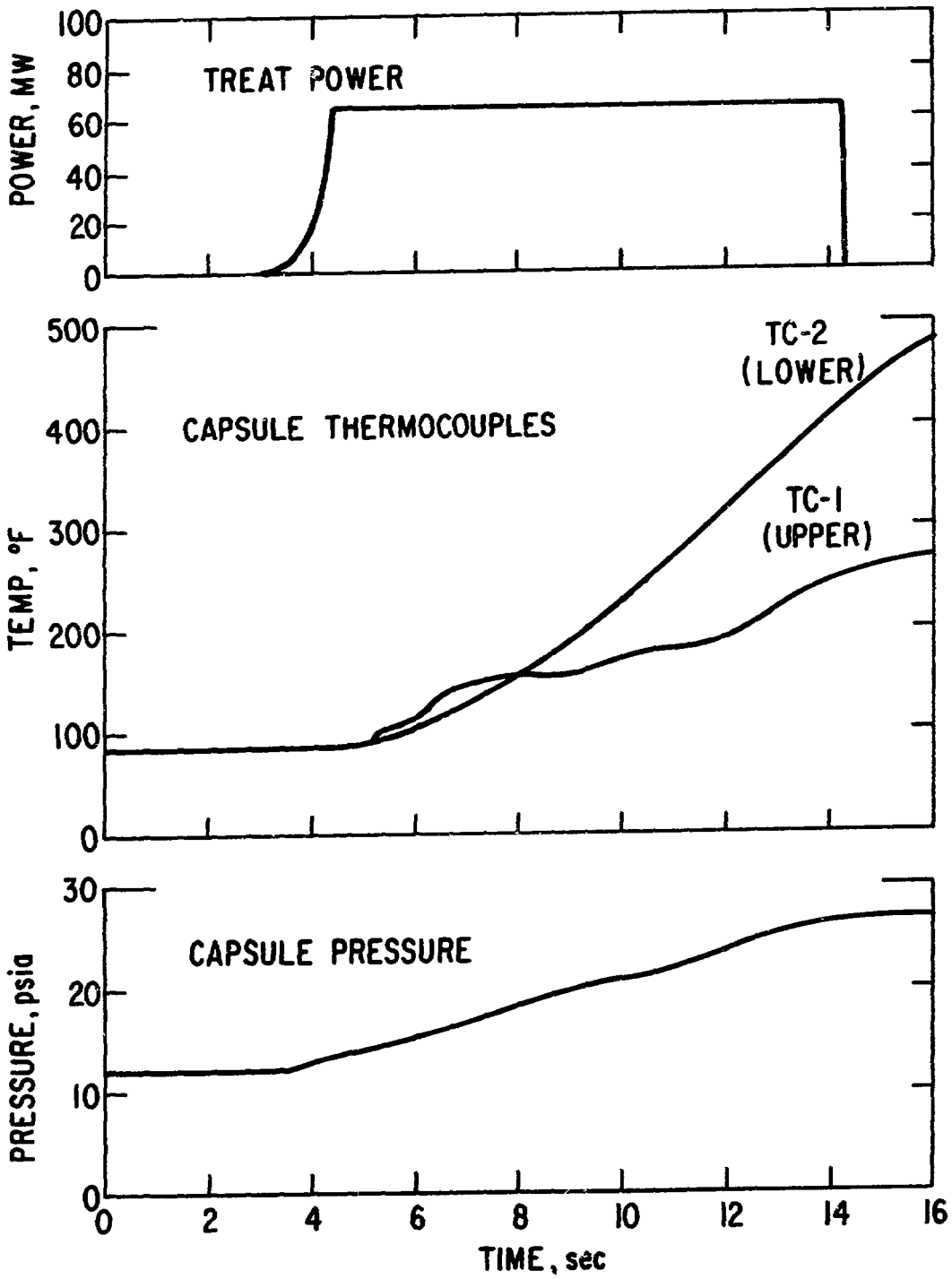

Fig. 8 F1 Test Data

Appendix A presents plots of raw test data that Fig. 8 is based upon. In addition, a plot of the thermocouple and pressure transducer data up to 120 sec after test initiation is included in Appendix A.

4.2 Posttest Neutron Radiography and Metallography

Fig. 9 is the posttest neutron radiograph of the F1 capsule. Pretest fuel column and heated-wall axial positions are shown for reference. The interpretation of the radiograph in Fig. 9 was aided by metallography performed on selected sections of the F1 test capsule. Final axial relocation of the fuel was downward, as evidenced by a 6 in. region voided of fuel above a 5 in. region of molten fuel. The molten fuel extends radially to the inside of the heated wall. Partially melted fuel segments exist above and below the regions of extensive axial relocation. Note that unmelted fuel pellets are found near the cooler end of each partially melted segment. A single unmelted fuel pellet at the top of the fuel column is the only fuel found above the original fuel column position after the test. Examination of the radiograph shows that the heated wall contained the test fuel adequately, as can be judged by its undeformed appearance and almost total confinement of the fuel within the inner diameter of the heated wall. What appears to have been molten fuel leaking out of the heated wall in one location near the top of the original fuel column is the only significant heated-wall breach.

Preliminary posttest metallography is available. The posttest metallography provides a large amount of information on the final condition of the fuel. Many more metallographic sections will be prepared, especially from the 5 in. region of molten fuel shown in Fig. 9, so any conclusions drawn from the preliminary metallography are subject to change. Information on the progression of events leading to gross axial fuel motion in the high power fuel originally at the fuel column mid-axis may be inferred by studying metallographic sections

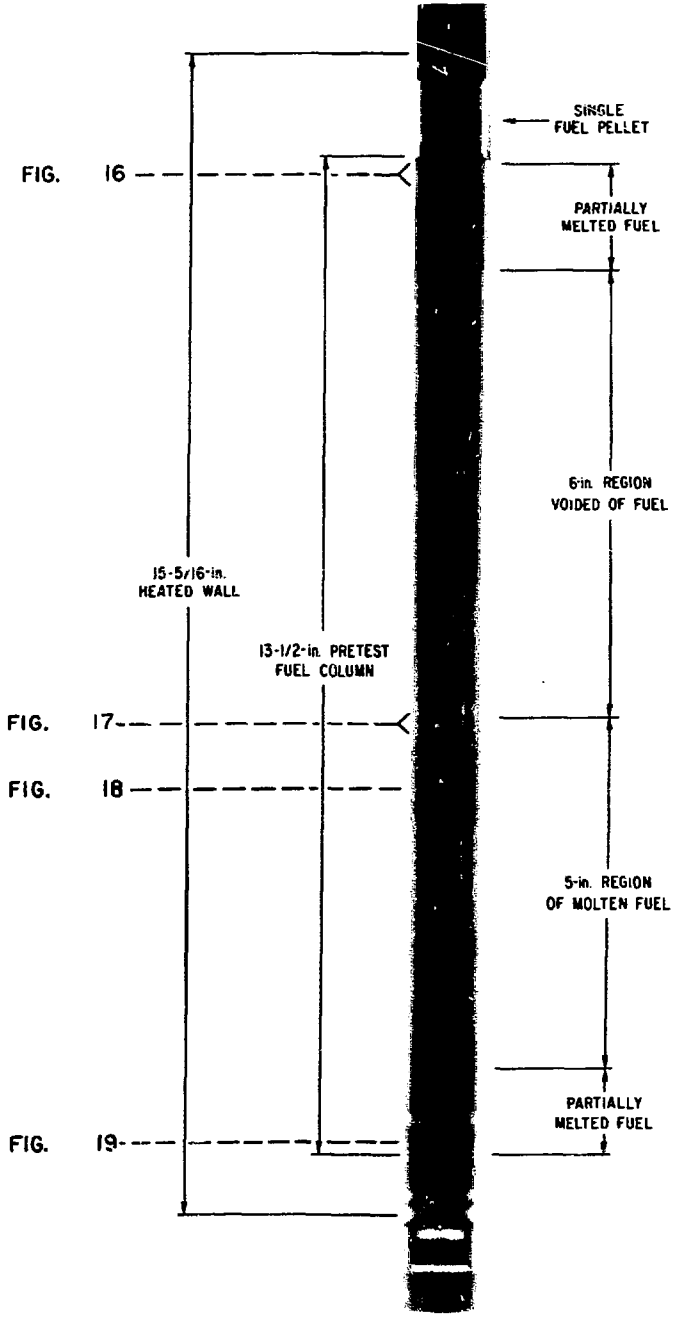

Fig. 9 F1 Posttest Neutron Radiograph

of the lower power fuel that had just started to swell and melt at the end of the test. Four sections prepared from the F1 test capsule are available and are presented in Figs. 10 through 13. The approximate test capsule locations of Figs. 10 through 13 are indicated in Fig. 9.

Fig. 10 shows the axial progression of fuel melting and swelling in the second and part of the third pellets from the top of the pretest fuel column. The pellet interface and the upper surface of the top pellet are indicated in Fig. 10 for orientation. Evidently power generation was terminated just before these pellets were to undergo gross axial fuel motion. Near the top of the second pellet very little change in pellet microstructure or dimensions occurred except for a slight amount of swelling in the unrestructured fuel. The axial power shape (Fig. 6) of the F1 test kept the fuel at the top of Fig. 10 at a lower temperature than the bottom. Note that the unrestructured fuel on the right side of Fig. 10 exhibits more swelling than the left side. This suggests that the right side of the pellet was hotter, and that there was a general azimuthal variation in temperature. The outline of the pellets in the neutron radiograph (Fig. 9) shows that one side of the top pellet was not centered axially within the heated wall; such an uncentered condition could cause an azimuthal temperature variation in these pellets. Swelling in the top pellet was 20% in both the radial and axial directions implying that fuel swelling was isotropic until contact with the heated wall. There are two large pores in the lower right side of Fig. 10 that were inadvertantly filled with a mixture of stainless steel cutting debris and epoxy during the metallographic section preparation. Only a very small number of barely visible metallic particles observed in Fig. 10 are though to be in the fuel as a result of prior irradiation (metallic fission products) or the F1 test (stainless steel clad). No evidence of stainless steel clad entering along cracks on the

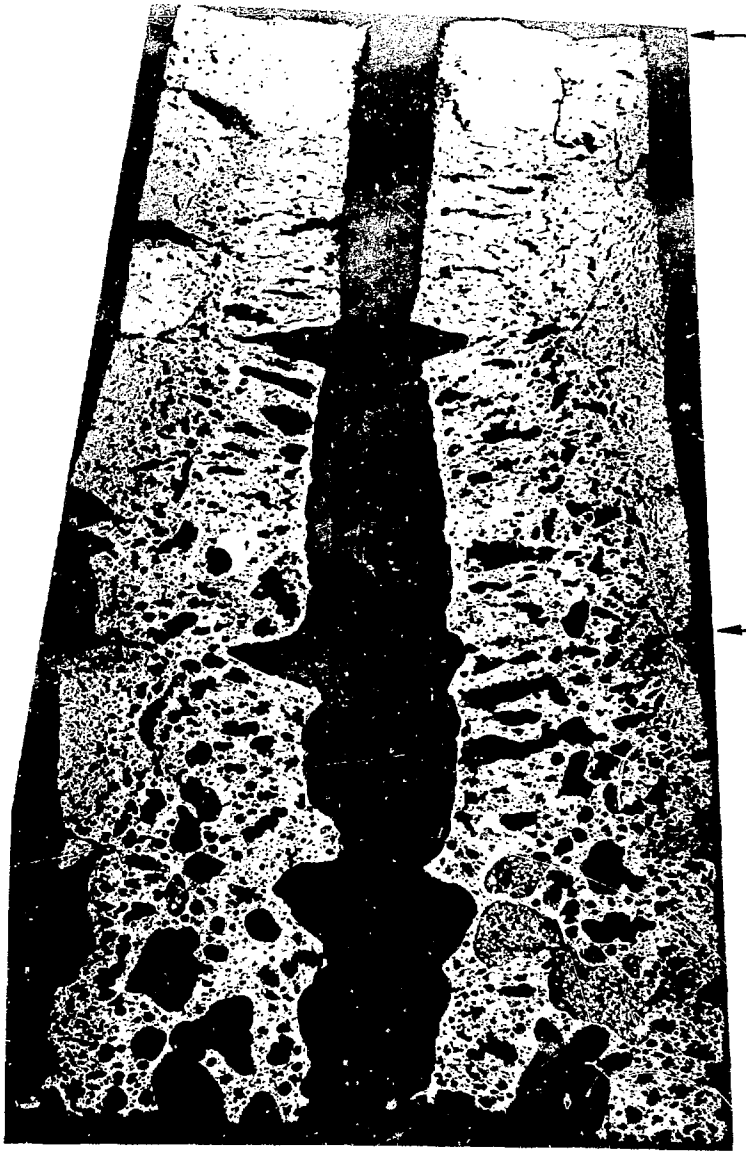

Fig. 10 Axial Progression of Fuel Swelling and Melting Along Two Pellets Near Top of Original Fuel Column. Magnified ~15 times

outside of the fuel pellets is apparent. As one proceeds downward axially and inward radially the porosity shape in Fig. 10 becomes less angular and assumes a more rounded shape. This change in porosity implies that at least the fuel solidus temperature was attained in regions of less angular porosity. The bottom of the lower pellet in Fig. 10 had swollen to 1.47 times its pretest diameter; an increase to 1.55 times the pretest diameter is necessary for the fuel pellet to expand out to the inside diameter of the heated wall. The lower pellet in Fig. 10 was sliced through during the test capsule disassembly, and it is possible that the fuel just below the slice in Fig. 10 had swelled out to the heated wall inside diameter. Near the bottom of Fig. 10 there is an uneveness in the shape of the central void that suggests that molten, formerly columnar fuel had started to run down the central void.

Figures 6, 9, and 10 suggest a fuel motion scenario. Fuel motion was intiated in the middle of the fuel column and spread towards the ends due to the F1 axial power profile. Motion is initiated when a fuel pellet swelled isotropically until constrained radially by the heated wall. Then molten fuel in the upper half of the fuel column drained out of each pellet by running down the central void towards an axial region almost completely voided of fuel. This molten fuel collected in a molten fuel region below the voided region. Molten fuel motion after fuel melting in the lower half of the original fuel column is less certain since drainage down the central void would be blocked due to filling the central void of the unswelled pellets below with molten fuel. For a fuel element near the center of an FFTF subassembly with fuel swelled out to the inside clad diameter, the fuel occupies 44.4% of the area within the coolant channel perimeter. Before the F1 test, the fuel occupied 41.3% of the cross-sectional area inside the heated wall. Thus swelling in the F1 test sufficient to cause a radial swelling constraint prior to molten

fuel motion implies that a similar situation might occur in FFTF under similar transient conditions. Note that the fuel motion scenario assumes that fuel swelling is sufficent to insure a radial constraint by the heated wall prior to molten fuel axial motion occurs at all levels in the fuel column. As a result of prior irradiation in EBR-II, the fuel near the ends of the fuel column had a greater fission gas content than fuel near the middle. This implies that less fuel swelling occurred in the middle of the fuel column before fuel melting was initiated.

Figure 11 is a section taken near the top of the 5 in. region of molten fuel identified in Fig. 9. The molten fuel and heated wall are labeled in Fig. 11 for orientation. Note that the heated wall sides are straight and seemingly unaffected by the F1 transient. No evidence of melting of the UO_2 phase in the heated wall has been observed. All the test fuel in Fig. 11 is believed to have been fully molten (above the liquidus) at the end of the F1 test. The large angular cracks found within the test fuel are believed to have formed after solidification following the F1 test. There is little evidence of gas or vapor bubbles in this fuel except for the one large round pore identified in the figure. The large center void in the middle of the molten fuel is not believed to be a remnant of the central void in the pretest fuel column. The void in Fig. 11 probably formed either by posttest fuel shrinkage during solidification from heat removal in the radial direction, or from a preference for molten fuel to run down the central void creating a type of miniscus. However, it is more likely that this is a solidification void. Note that the left side of the void is smooth which is consistent with formation by solidification. This suggests that the angular outline of the right side of the void is due to an inadvertent loss of fuel during specimen preparation, and Fig. 11 is a distortion of the true size and shape of the solidification void.

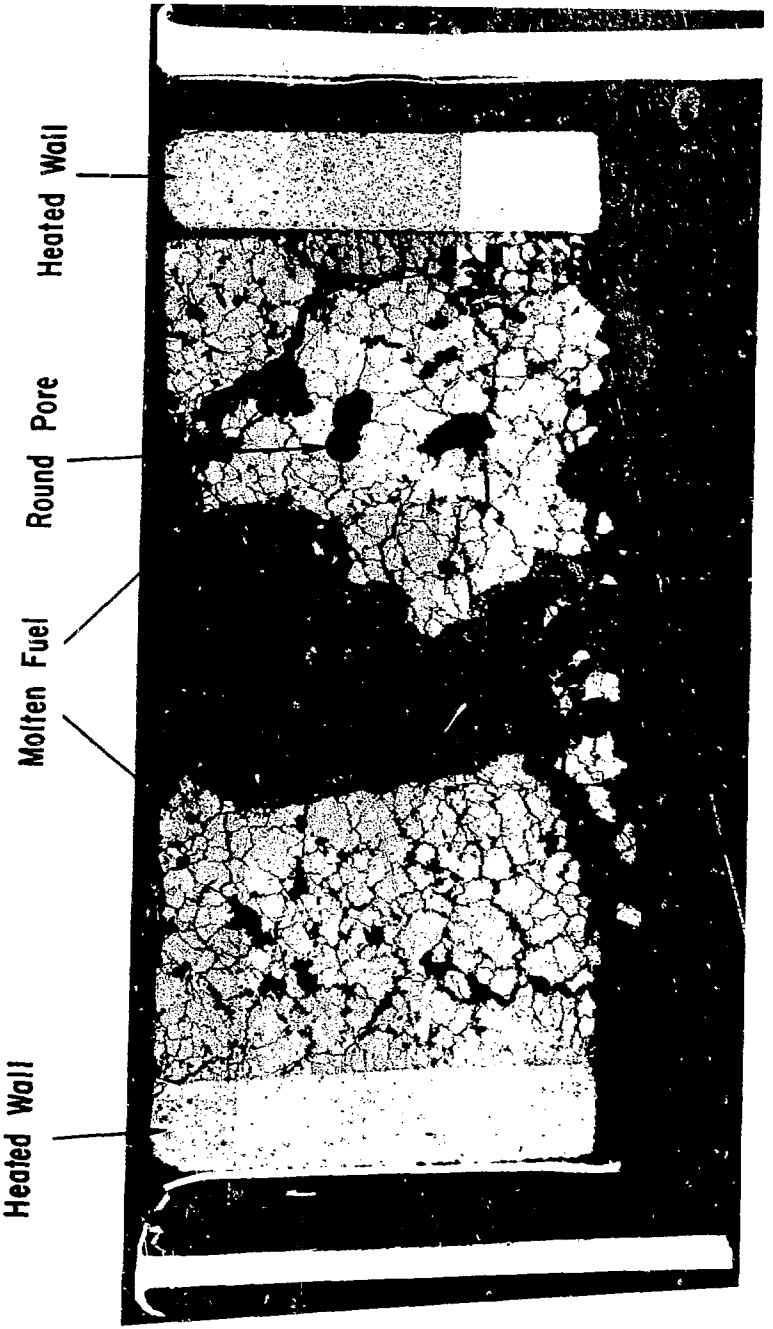

Fig. 11 Section Near Top of 5 in. Region of Molten Fuel
Magnified ∿18 times

Several particles of a light metallic phase are visible in Fig. 11. The smooth round shape of these particles suggests that they were once molten. No chemical identification of these metallic particles has yet been made.

Fig. 12 is a large metallic particle found in the 5 in. region of molten fuel about 2 in. below Fig. 11. No chemical identification of this particle has been made, but its large size (~90 mil diameter) suggests that it is too large to be a metallic fission product ingot in the fuel of this burnup. The dendritic microstructure is typical of stainless steel cladding. Further, there is evidence that this particle may be at least 1/2 in. long. How such a large particle of cladding arrived at this axial level is an interesting question. One goal of the F1 test was to completely drain the clad off the fuel column before gross axial fuel motion occurred. A large ingot of melted clad was indeed found near the bottom of the fuel column. Since the clad is less dense than the fuel, it is possible that the drained clad rose up through the molten fuel above it. The particle in Fig. 12 could be a drop of cladding rising up through the molten fuel that was frozen in place when the fuel solidified around it. Alternatively, it is possible that the particle in Fig. 12 is from clad that either rose up through the molten fuel or dripped down from the top of the fuel column and floated on top of the molten fuel. When the molten fuel solidified furing cool-down after the F1 test, the molten clad could have run down the central solidification void to solidify at the axial level of Fig. 12. A careful metallographic examination may resolve exactly how this particle of clad arrived at this axial level.

Fig. 13 is a section showing the bottom fuel pellet surrounded by clad that had drained down the fuel column. The heated wall surrounds the once molten clad. For orientation, the fuel, clad, and heated wall are identified in Fig. 13. Several radial zones of microstructure in the fuel are evident.

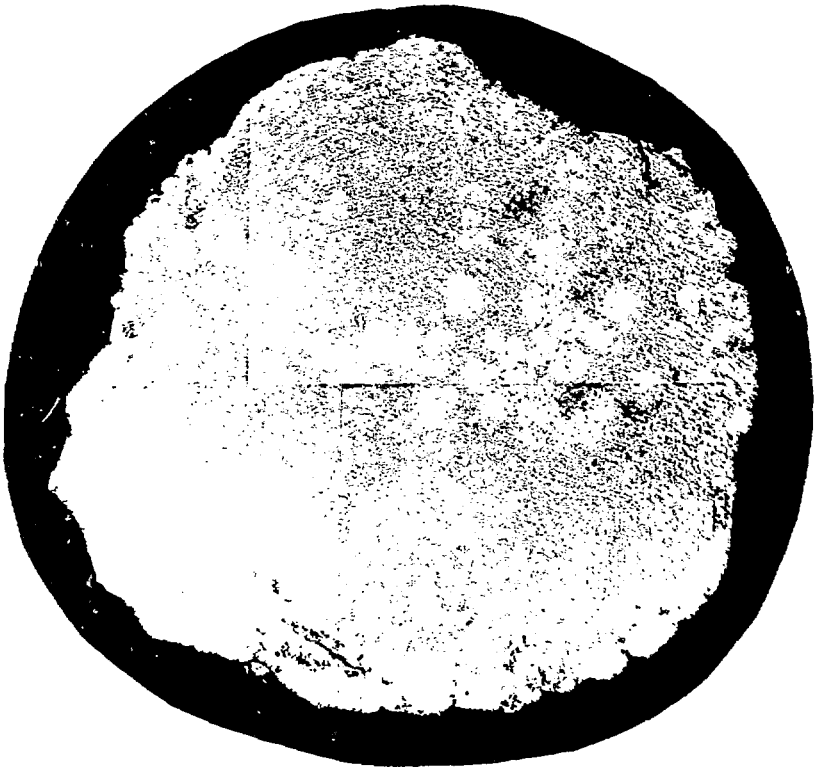

Fig. 12 Large Metallic Particle Found in 5 in. Region of Molten Fuel Magnified ∿50 times

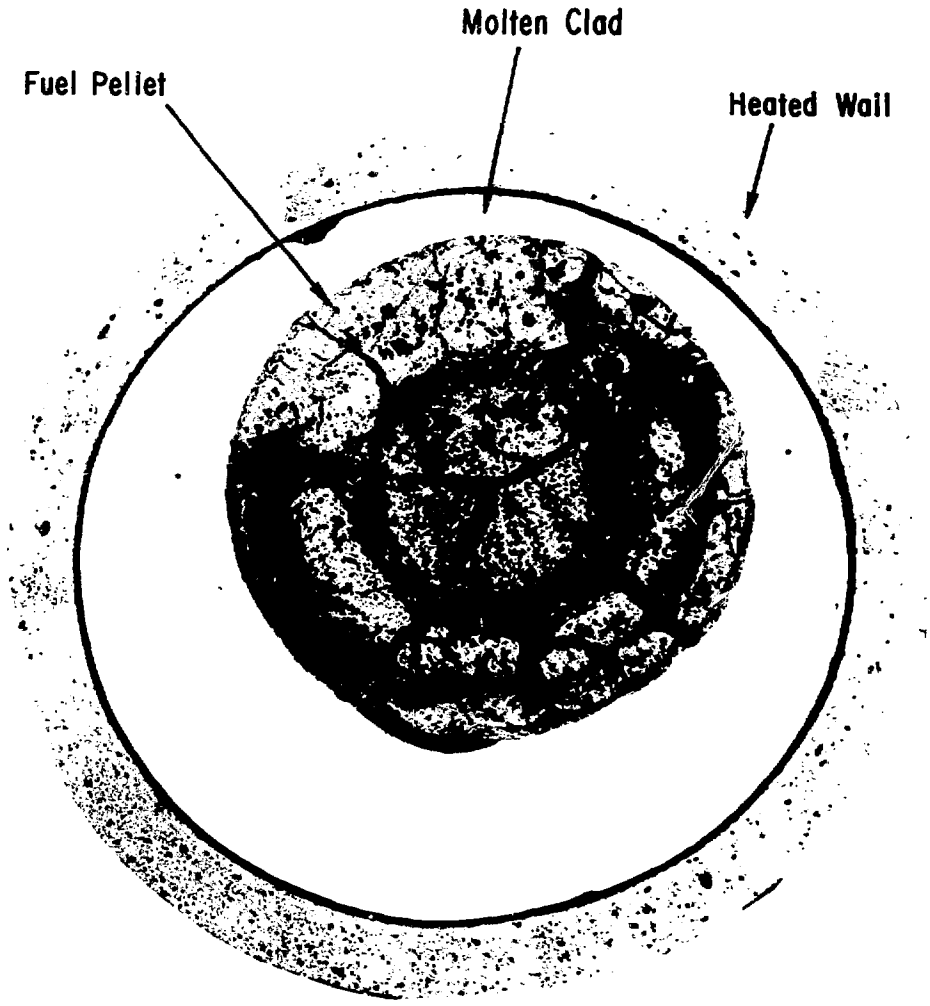

Fig. 13 Bottom Fuel Pellet Surrounded by Molten Clad
Magnified ∿16 times

Starting from the outside of the fuel the layers are:

1. A thin ∿4 mil layer of porous fuel exhibiting inter-granular swelling or cracking. The voids produced by the swelling or cracking are perpendicular to the pellet radius.
2. An unrestructured layer ∿15 mils thick. This layer is characterized by coarse porosity, cracks, and some swelling. Some of the cracks are partially healed and the regions next the cracks tend to be preferentially swelled.
3. An equiaxed layer of ∿17 mils thickness and ∿30 microns grain size. This layer has both coarse and fine porosity. The fine porosity exists both on grain boundaries and within the grain. This fine porosity may be due to transient fission gas release.
4. A foamy layer of ∿18 mils average thickness. Extreme swelling occurred in this layer from fission gas release in the F1 test. It is implied that this layer did not melt since the fuel inside and outside of this layer did not melt. As much as 300% swelling occurred in this fuel.
5. The central region of 184 mils diameter contains vestiges of columnar grains. No evidence of melting was observed in this region. The central fuel void did not extend down to this axial level.

Fig. 13 provides a lot of information of fuel response due to rapid heating. However, neither the fuel microstructure nor the radial temperature profiles in this pellet are typical of the rest of the fuel in the F1 test.

4.3 Hodoscope Results

A preliminary analysis of the hodoscope data show that starting about 1 sec before scram, there is a slow loss of fuel from the top half of the fuel pin. It should be emphasized that this is only a preliminary

hodoscope analysis, and a more detailed analysis will be included in the F1 final report.

Due to the presence of the nuclear-heated wall, the signal-to-background ratio of the F-series fuel pin was reduced compared to previous single fuel pin tests conducted without heated walls. For a single fuel pin without a heated wall observed by the hodoscope along a half reactor slot, a signal-to-background ratio of 3.5 is achievable. Since both the test fuel and the nuclear heated wall generate neutrons in the F-series, the effective signal-to-noise ratio for the test fuel was reduced to 1.5 as determined by F1 count-rate profiles.

A series of hodographs (see Fig. 14) has been produced showing the time history of the fuel pin during the transient. The pin appears to maintain a ramrod-straight appearance until close to scram, when it becomes apparent that fuel has been lost from the top half.

The fuel loss can be pinpointed more quantitatively by examining the series of axial profiles in Fig. 15. These profiles represent averages taken over an interval of 200 msec, except for six such profiles combined into an average over the postscram period of 14.24 to 18.50 sec. At 13.04 sec, the distribution appears within statistical fluctuations to be consistent with earlier profiles in an intact pin. At 13.24 sec, there may be the first evidence of fuel loss at the top third of the pin. This fuel loss generally continues through the remaining intervals, becoming fairly marked after scram. In general, the fuel loss may have been initiated at 13.1 $\pm$ 0.1 sec and terminated some seconds after scram.

The loss appears to have been gradual, with at least half the loss in the 1 second interval before scram and the other half afterward. Fig. 14 indicated that fuel was lost from about two-thirds of the upper half of the fuel

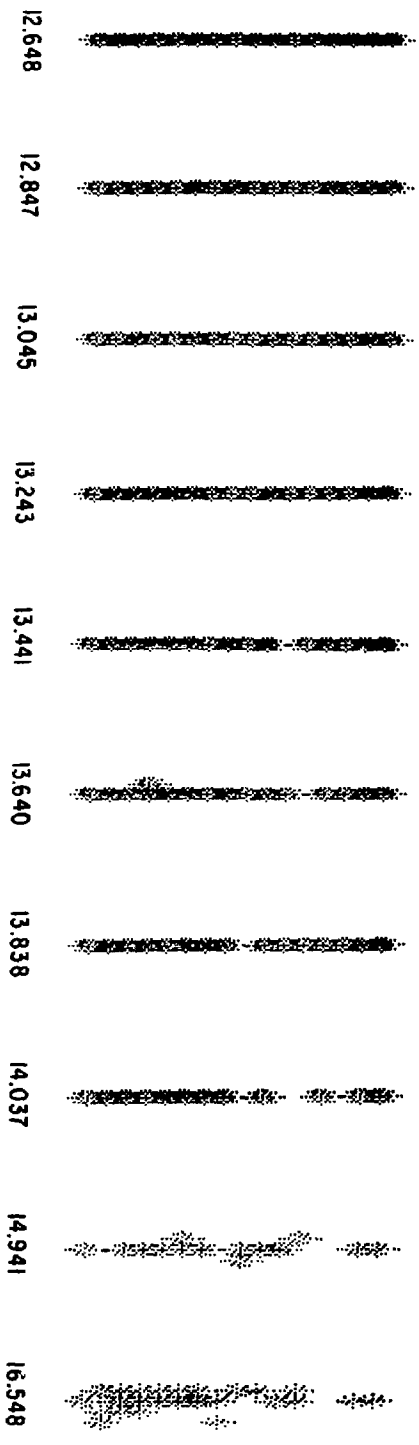

Fig. 14 Hodographs from Test F1

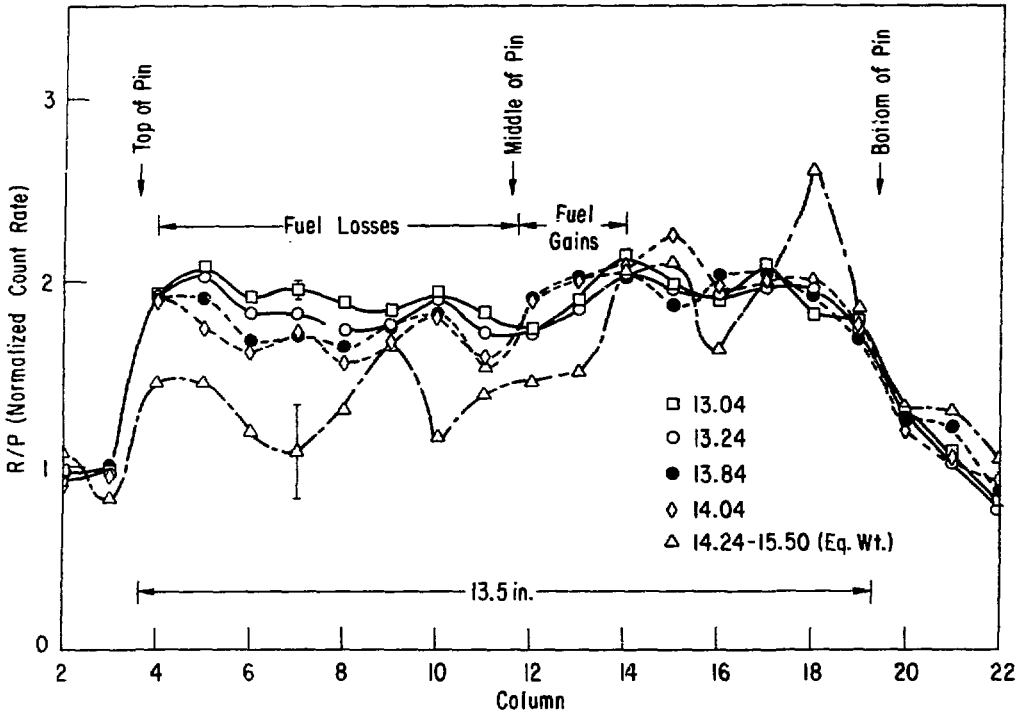

Fig. 15 F1 Axial Fuel Profile from Hodoscope

column. These interpretations must be qualitative at this stage, particularly because of the large statistical uncertainty (indicated by the typical error bars) of the postscram data.

There is some evidence of limited slumping to a region just below the midplane; otherwise there is little statistically clear sign of fuel having drained. No significant increase in the fuel density appears to have taken place in positions near the ends of the original fuel column.

5.0 THERMAL AND FUEL MOTION ANALYSIS

Calculations of fuel temperature and fuel motion for test F1 were performed using the SAS code[2].

Fig. 16 presents the test fuel radial temperature profiles calculated for various times during the F1 test for the fuel segment at mid-axis. As is shown by reference to the axial power profile in Fig. 6, the fuel at mid-axis is the hottest fuel in the F1 test up until the time of gross axial fuel motion. SAS considers fuel thermal expansion, so the radial temperature profiles in Fig. 16 are plotted versus a fractional radial abscissa. Since the F1 test starts at room temperature, the initial radial temperature profile is flat. By 5.0 sec (just after attaining constant TREAT power) a parabolic temperature profile has been obtained. The temperature gradient becomes steeper due to heat transfer to the clad until about 9.4 sec. Finally the clad melts off of the fuel column, and by 11.6 sec the radial temperature gradient has decreased. A SAS calculation of the radial temperature profile at 12.8 sec is also presented in Fig. 16. At 12.8 sec the fuel solidus temperature has almost reached the unrestructured fuel. Beyond 12.8 sec the fuel at mid-axis is considered by the SLUMPY analysis.

Calculation of axial fuel motion using the SLUMPY[3] module of the SAS III-A code was made for the F1 test. Initiation of the SLUMPY calculation was made when the fuel melt zone* reached the unrestructured fuel. Figs. 17, 18, and 19 graphically report the SLUMPY calculation at initiation of SLUMPY, reactor power termination, and about 1 sec after power termination respectively. Note that the initiation time of the SLUMPY calculation (12.82 sec) is close to the time the hodoscope detected axial fuel motion (13.2 sec).

---

*Fuel outside melt zone has not started to absorb the heat of fusion.

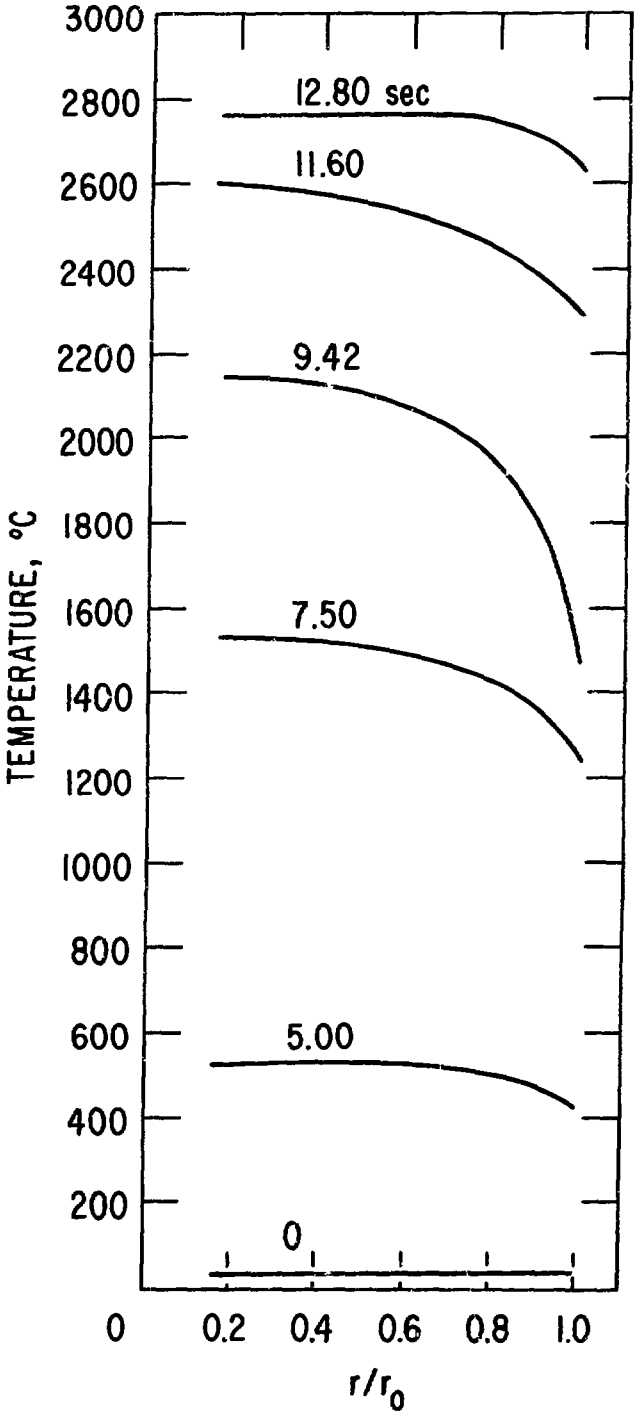

Fig. 16 SAS Calculation of F1 Test Fuel Radial Temperature Dependence at Fuel Mid-Axis

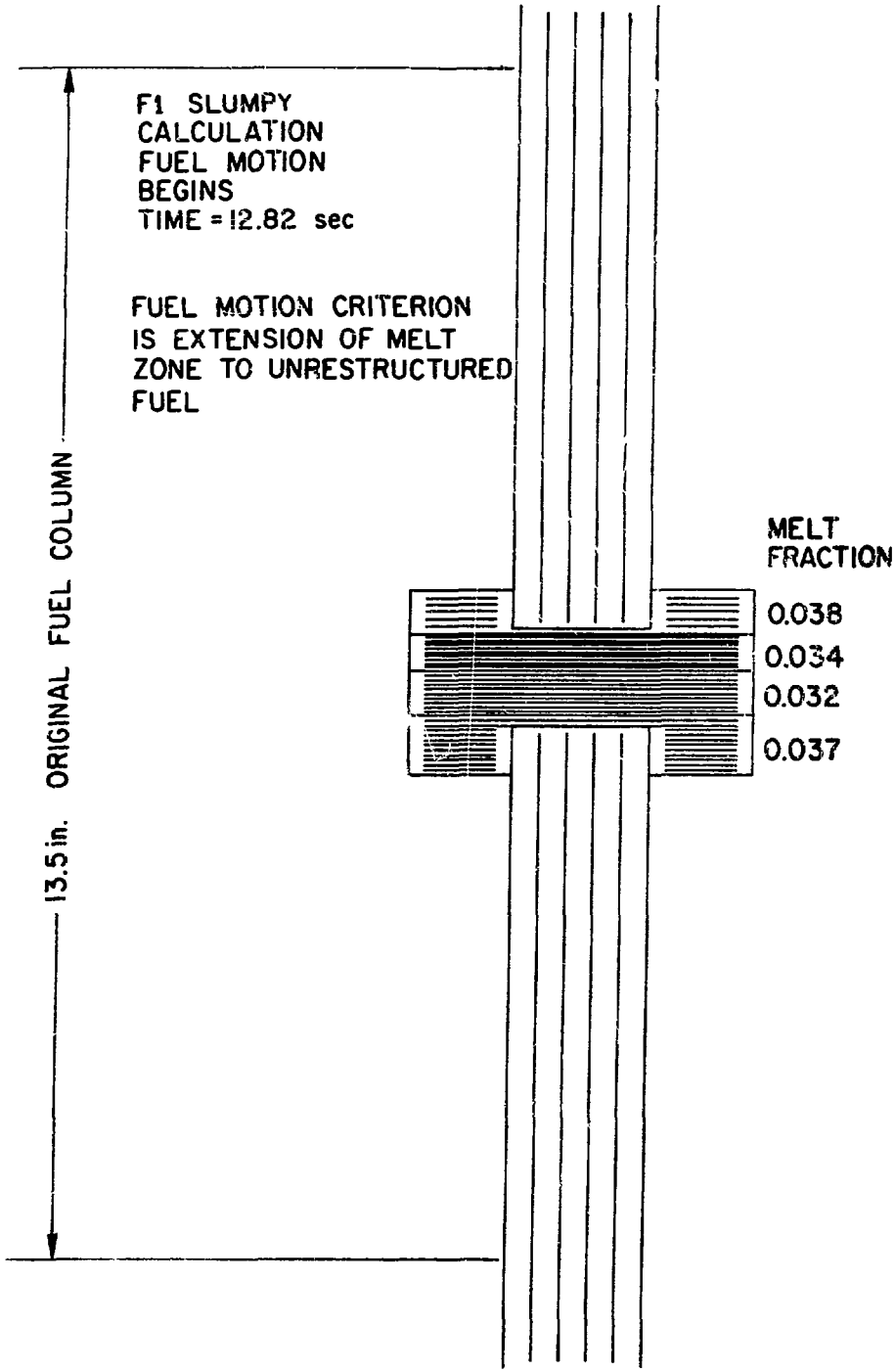

Fig. 17 F1 SLUMPY Results at 12.82 Sec.

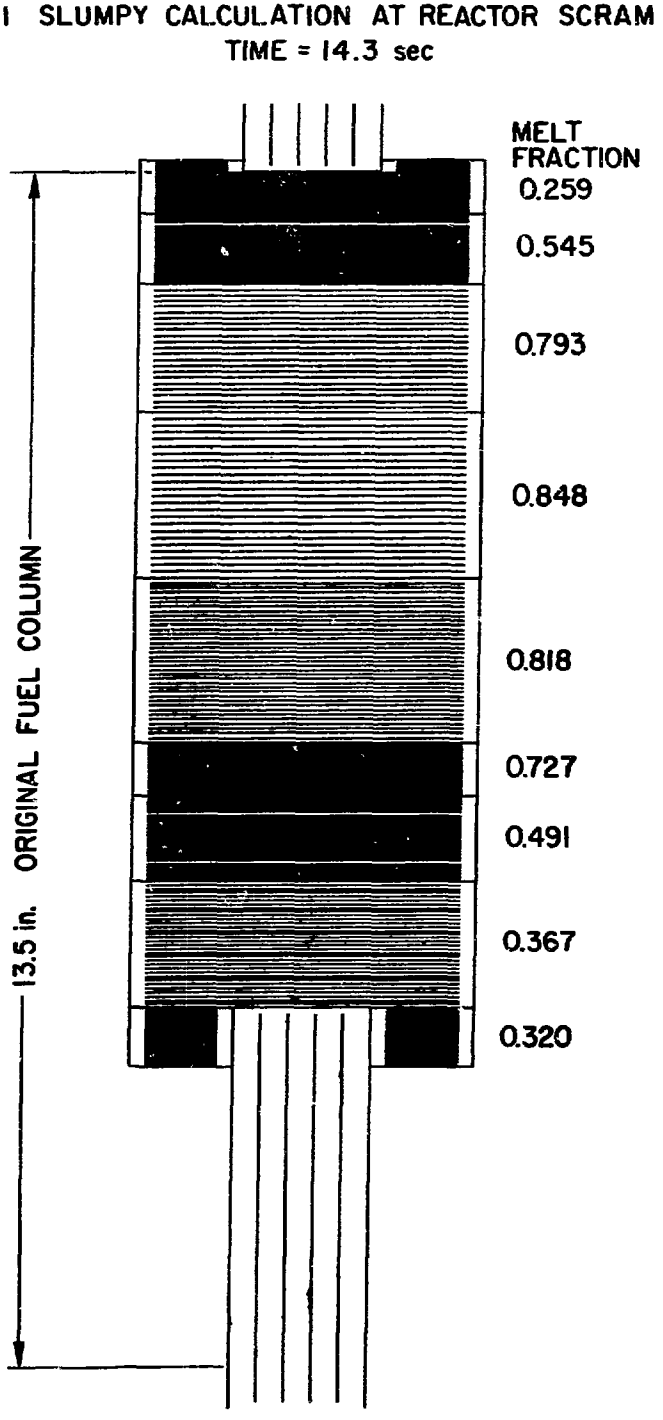

Fig. 18 F1 SLUMPY Results at 14.3 Sec.

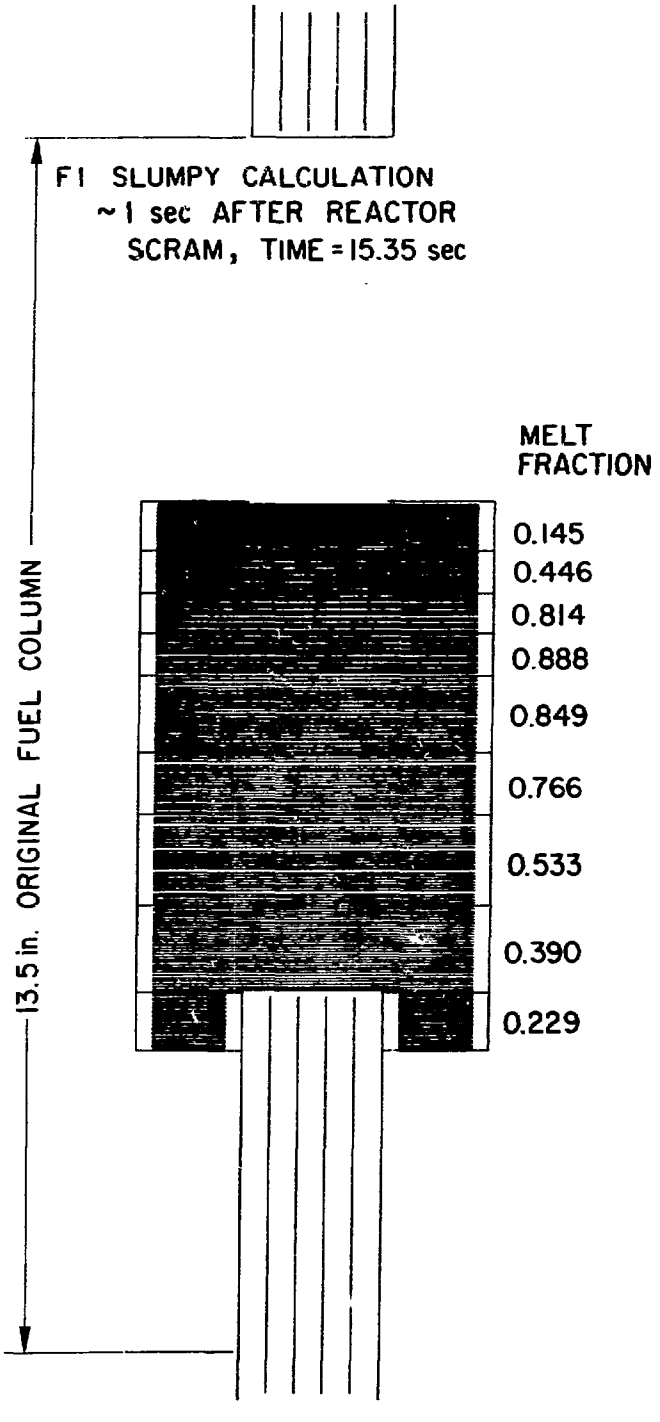

Fig. 19 F1 SLUMPY Results at 15.35 Sec.

SLUMPY models fuel motion with a central compressible region of fission gas, solid fuel, and molten fuel. This compressible region is assumed to have a diameter equal to that of the inside of the heated wall. Relative densities of the nodes within the compressible region are indicated by the degree of shading in Figs. 17, 18, and 19. Melt fractions* of these nodes are also shown in these figs. Axial segments of fuel above and below the central compressible region are also indicated in these figures with vertical shading. These upper and lower segments represent fuel that has not met the criterion for SLUMPY initiation. Initiation of the SLUMPY calculation is in the mid-axis of the fuel column as shown in Fig. 17. Note that this mid-axis fuel generates the most power as indicated by the axial power profile in Fig. 6. By reactor scram time (Fig. 18) the compressible region has grown to include the upper two-thirds of the fuel column. After about 1 sec after reactor scram, the compressible region has collapsed to occupy the central one-third of the original fuel column as indicated in Fig. 19. The upper one-third of the original fuel column is voided and the lower one-third has not yet met the SLUMPY criterion for initiation of the compressible region calculation as shown in Fig. 19. A comparison of Fig. 19 and the posttest neutron radiograph (Fig. 9) show good qualitative agreement. The SLUMPY calculation is sensitive to input assumptions such as energy deposition after axial fuel motion begins, fuel viscosity, and fuel fission gas concentration. Details of the input assumptions and a revised SLUMPY calculation, partially based on information generated in the posttest metallographic examination, will be presented in the final report.

---

*Fraction of fuel that has absorbed the heat of fusion.

6.0 PRELIMINARY CONCLUSIONS

The following conclusions can be made based upon the posttest neutron radiograph; and incomplete hodoscope and posttest metallography results:

1. Retained fission gas did not prevent an axial fuel collapse in test F1.
2. Retained fission gas did not cause any gross axial dispersion of fuel prior to the collapse in test F1.
3. The nuclear heated wall provided good test fuel radial boundary conditions in test F1.

REFERENCES

1. F. L. Yaggee and G. Dragel, An Ultrasonic Trepanning Technique for Radial Sampling of Ceramic Fuel Pellets for Fission Analysis, Trans. Am. Nucl. Soc., 19, 263 (1974).

2. M. G. Stevenson, W. R. Bohl, F. E. Dunn, T. J. Heames, G. Hoppner, and L. L. Smith, Current Status and Experimental Basis of the SAS LMFBR Accident Analysis Code, Proceedings of the Fast Reactor Safety Meeting, Beverly Hills, California, 1303 (1974).

3. W. R. Bohl and M. G. Stevenson, A Fuel Motion Model for LMFBR Unprotected Loss-of-Flow Accident Analysis, CONF-730414-P2, Ann Arbor, Michigan (April 1973).

APPENDIX A

F1 Test Data

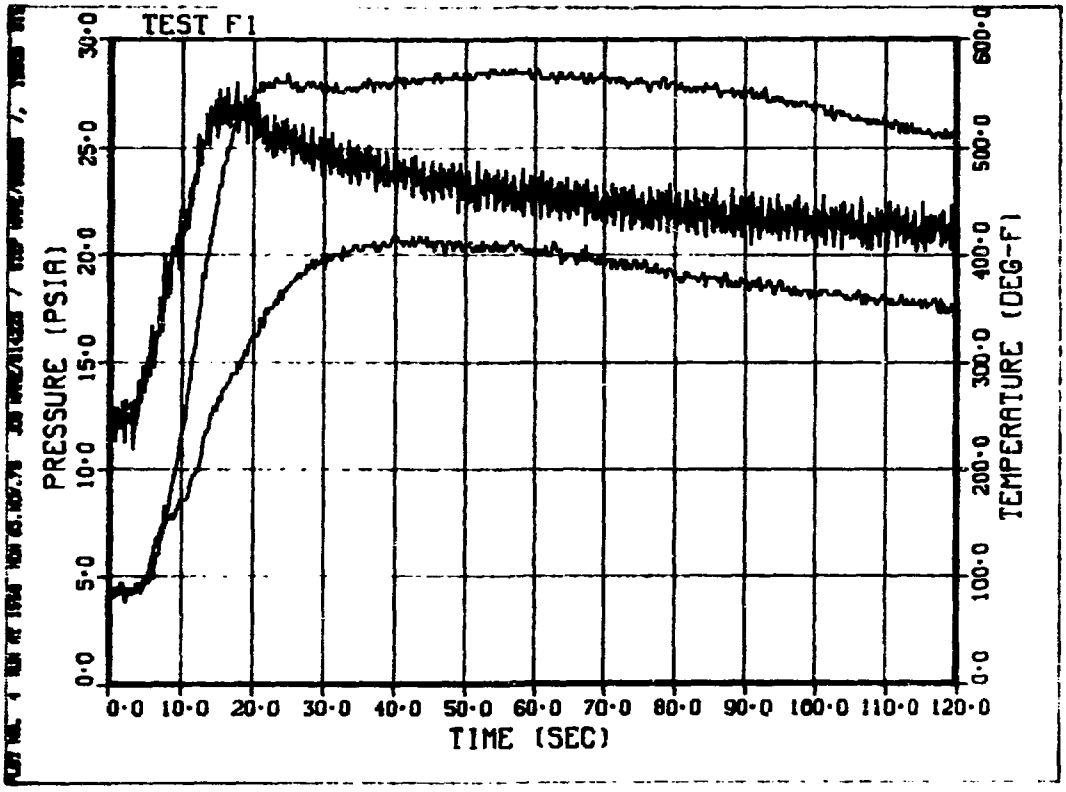

Fig. A1 Pressure and Temperature Data

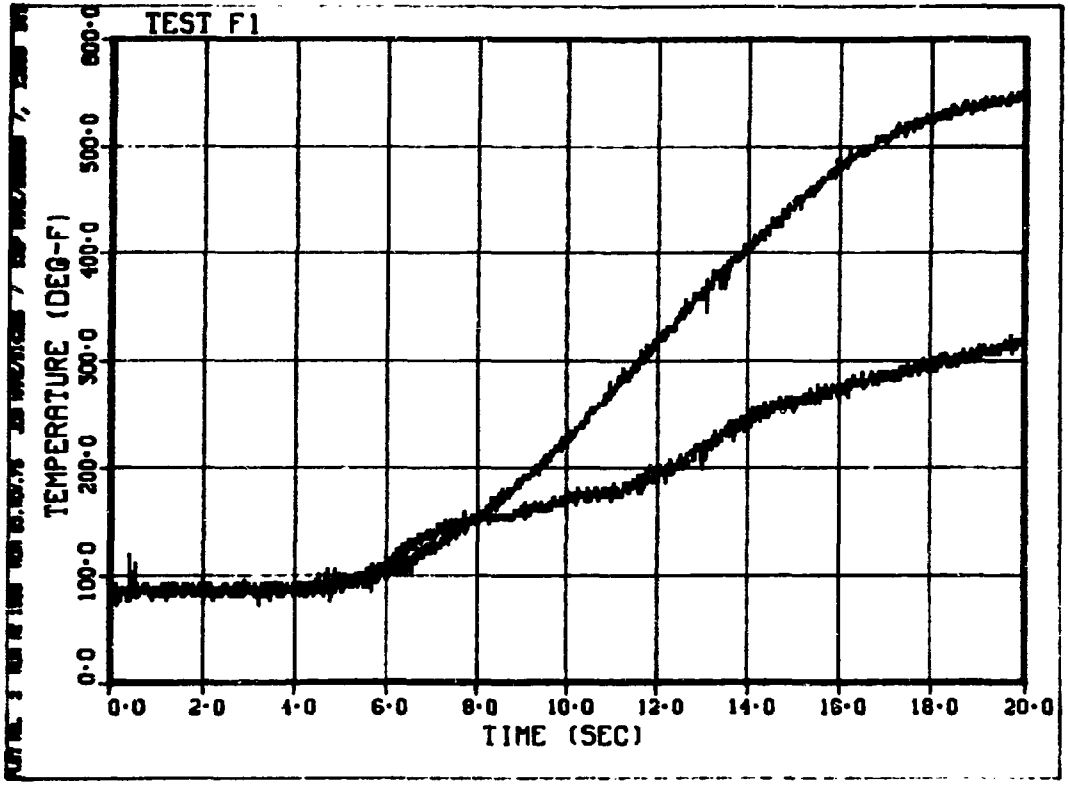

Fig. A2 Thermocouple Data

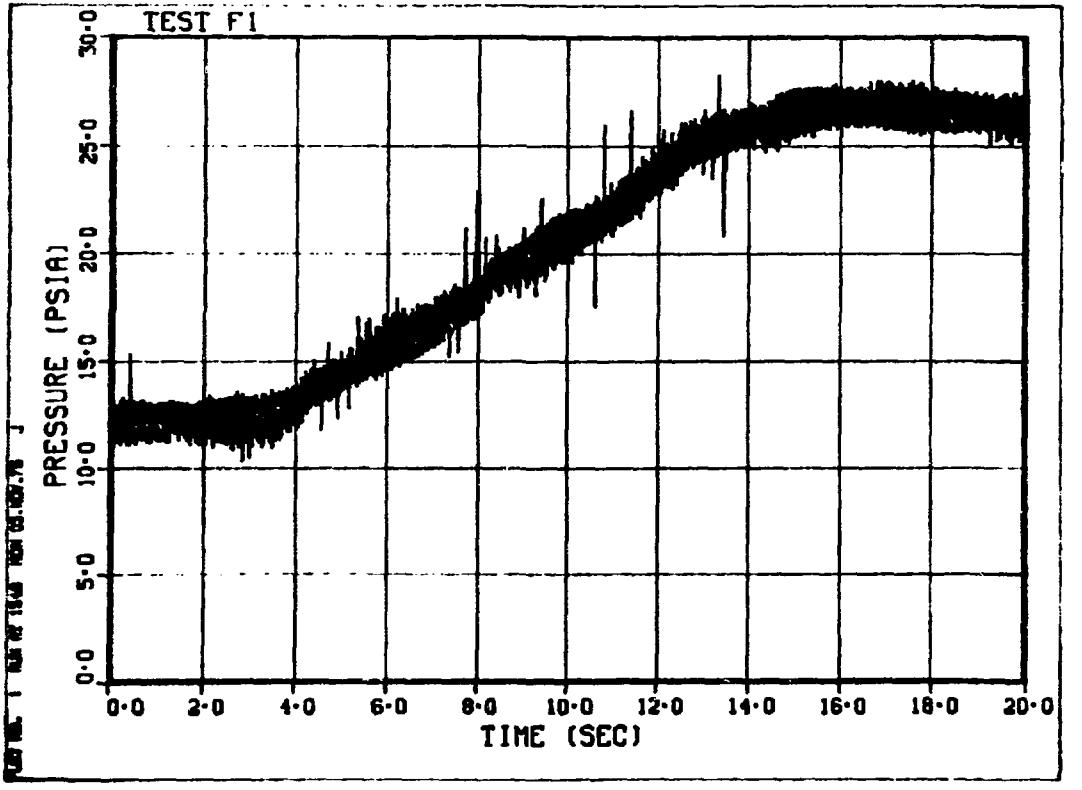

Fig. A3 Pressure Transducer Data

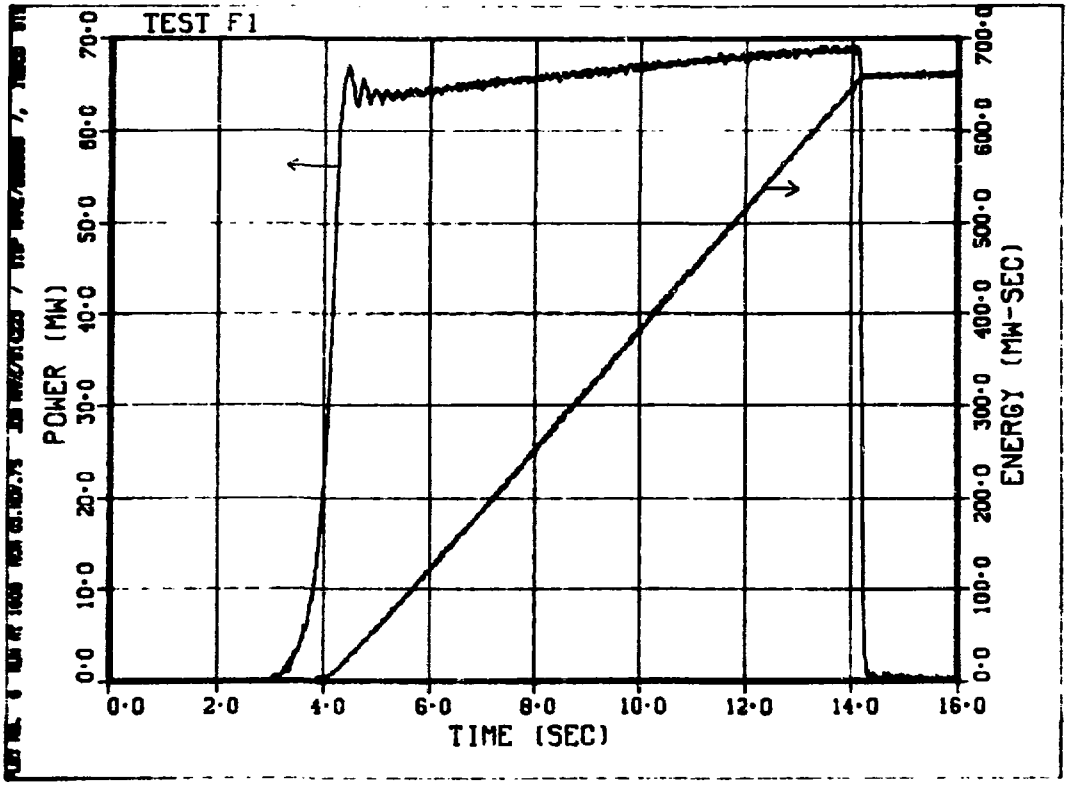

Fig. A4 Reactor Power (Safety #1) and Energy (Integrator #1)

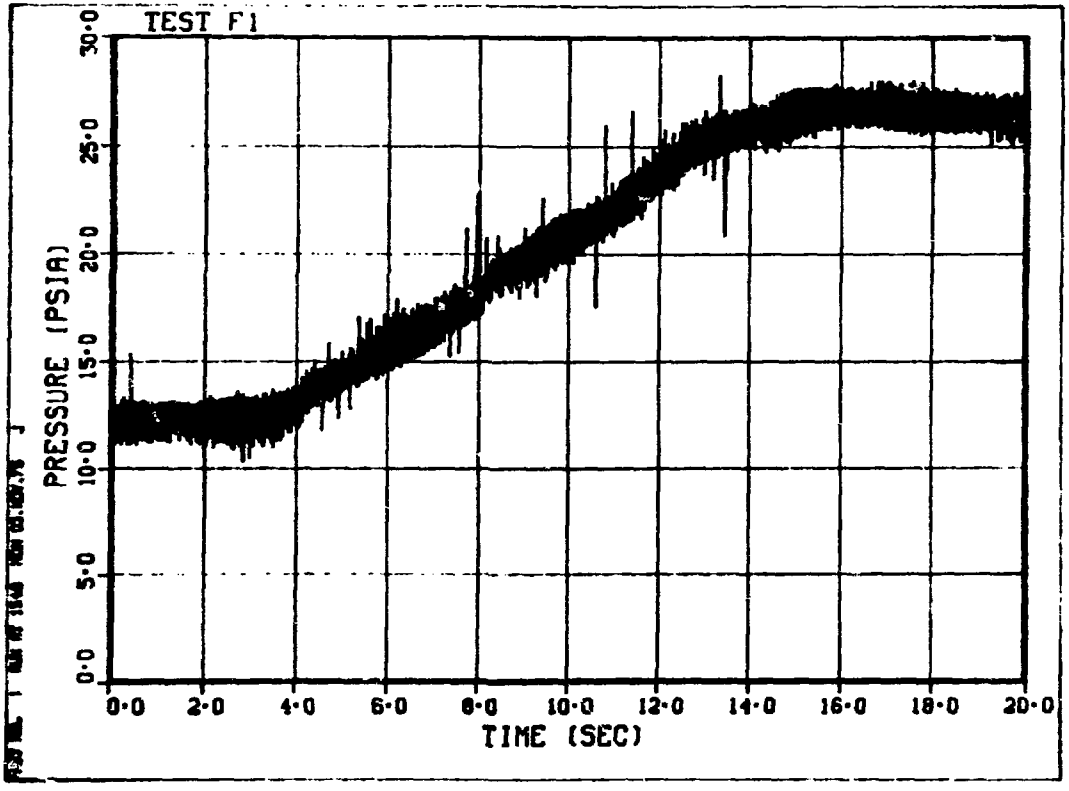

Fig. A3 Pressure Transducer Data

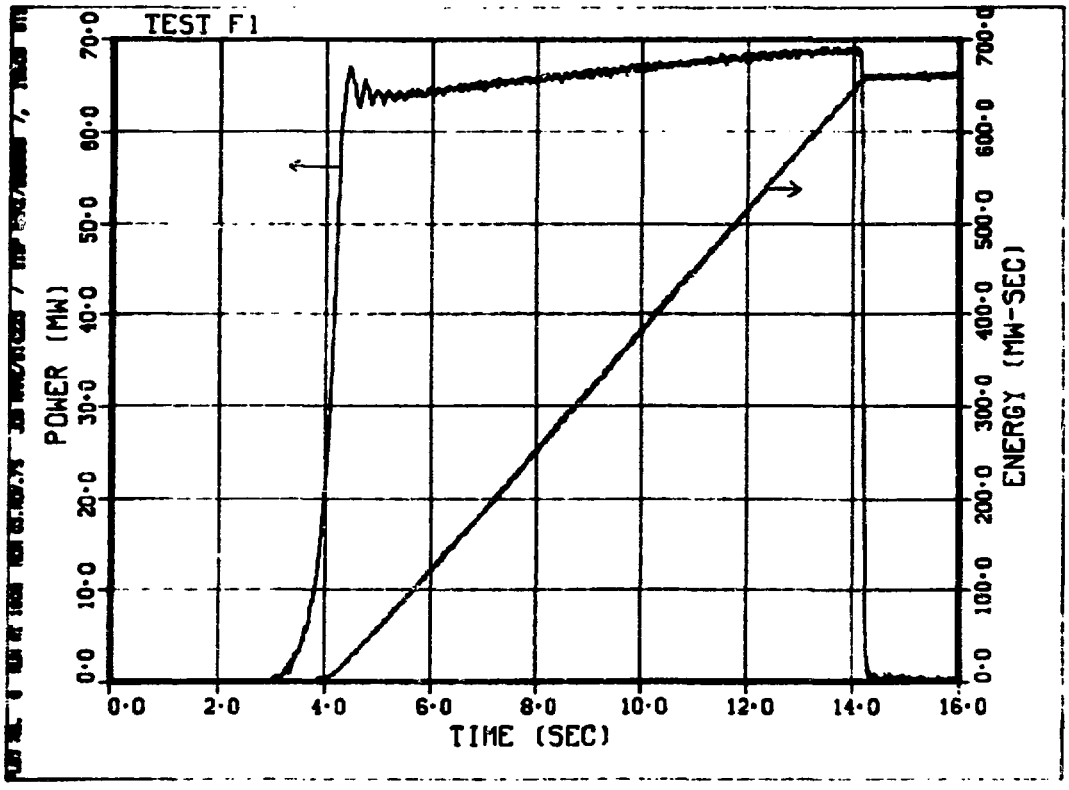

Fig. A4 Reactor Power (Safety #1) and Energy (Integrator #1)

ACKNOWLEDGEMENTS

The execution of the F1 test and the F-series power calibration tests depended on contributions from many persons at Argonne. The overall direction of the program was the responsibility of Charles Dickerman. Bob Noland was responsible for test hardware and experiment operations. Larry Harrison, at TREAT, provided the facility management for running the test.

Special mention must be given to Chuck McPheeters and Verne Kolba, who served as lead experimenter and test designer respectively, during the conceptual and power calibration stages of the F-series.

Paul Basnar assisted in design of the F-series and also created the engineering drawings. Operations Group Leader, Neill Carson, and Test Engineer, Dick Purviance, supervised the assembly of the F-series hardware. Jim Emerson assembled the F-series test trains. Special mention to Paul Basnar, Neill Carson, Dick Purviance, and Jim Emerson is in order for making last minute changes in the test design and still meeting the schedule. Gene Maslowicz and Joe Burghardt outfitted the F-series Mark II-A loops. Ken Schmidt, Jerry Dewey, Charley August, and Bob Mailhoit also assisted with the F-series hardware. Lindy Willis handled the shipping of the test hardware between Illinois and Idaho. Fuel and HFEF coordination was handled by Howard Rhude. George Trahey and Lew Garrison were the Q/A representatives. Typing of this report was by Rosie Tooley. Pam Parks, Liz Rooney, Barbara Cobb, and Kathy Rank typed the volumes of information needed to execute the F-series tests.

Mark Stephenson performed many heat transfer and reactor kinetics calculations for the F-series. Mark also wrote the F-series safety report. Gerry Klotzkin and Jack Ulrich performed Monte-Carlo and transport neutronic

calculations for the F-series. Frank Yaggee, Gabe Dragel, and Roland Armani devised and executed an experimental method of obtaining the radial power profile used for the F-series. Extensive radiochemical work for the calibration tests was performed by Earl Ebersole and Bob Villareal. Earl Ebersole was also quite helpful in explaining the precision and accuracy that could be expected from the radiochemical determinations. Paul Froehle digitized the F-series data after the F1 and F2 tests and prepared the graphs of the raw test data.

At HFEF; Jay Cook, Ken Teraguchi, and Jim Kerr worked on the hot cell operations needed to assemble and disassemble the F-series tests. At TREAT, Bill Knapp as test coordinator was instrumental in the successful execution of all the F-series transients. Roger Conant assisted Bill Knapp. Gerry Larsen at TREAT worked on the reactor power control system. In addition, Gerry provided the experimenters with a first look at the F1 and F2 test data by digitizing the test data in the evening following each test. The entire operation staff at TREAT is acknowledged for their efforts.

Bill Kentman cut up the test capsule after the F1 test in the MSD alpha-gamma hot cell. Jeff Puro prepared the F1 metallographic specimens.